Developing a reliable strategy to infer the effective soil hydraulic properties from field evaporation experiments for agro-hydrological models

Kefeng Zhang[a*], Ian G Burns[a], Duncan J Greenwood[a], John P Hammond[a], Philip J White[b]

[a]Warwick HRI, The University of Warwick, Wellesbourne, Warwick, CV35 9EF, UK
[b]Scottish Crop Research Institute, Invergowrie, Dundee, DD2 5DA, UK

[*]Corresponding author

Address: Warwick-HRI, The University of Warwick, Wellesbourne, Warwick CV35 9EF, UK
Tel: 0044 24 7657 4996
Fax: 0044 24 7657 4500
E-mail: kefeng.zhang@warwick.ac.uk

No of text pages: 25
No of figures: 10
No of tables: 2

Abstract

The Richards equation has been widely used for simulating soil water movement. However, the take-up of agro-hydrological models using the basic theory of soil water flow for optimizing irrigation, fertilizer and pesticide practices is still low. This is partly due to the difficulties in obtaining accurate values for soil hydraulic properties at a field scale. Here, we use an inverse technique to deduce the effective soil hydraulic properties, based on measuring the changes in the distribution of soil water with depth in a fallow field over a long period, subject to natural rainfall and evaporation using a robust micro Genetic Algorithm. A new optimized function was constructed from the soil water contents at different depths, and the soil water at field capacity. The deduced soil water retention curve was approximately parallel but higher than that derived from published pedo-tranfer functions for a given soil pressure head. The water contents calculated from the deduced soil hydraulic properties were in good agreement with the measured values. The reliability of the deduced soil hydraulic properties was tested in reproducing data measured from an independent experiment on the same soil cropped with leek. The calculation of root water uptake took account for both soil water potential and root density distribution. Results show that the predictions of soil water contents at various depths agree fairly well with the measurements, indicating that the inverse analysis is an effective and reliable approach to estimate soil hydraulic properties, and thus permits the simulation of soil water dynamics in both cropped and fallow soils in the field accurately.

Key words: inverse analysis, soil hydraulic properties, Genetic Algorithm (GA), soil water dynamics, root water uptake.

1. Introduction

The prediction of soil water movement is a central feature of agro-hydrological models. However, the treatment of soil water dynamics in many of these models is often approximate as they do not rely on basic flow theory (Ritchie, 1998; Droogers et al., 2001; Zhang et al., 2007, 2009; Renaud et al., 2008; Pedersen et al., 2009; Rahn et al., 2009). Many adopt the cascade approaches for hydrological simulations. According to the reviews by Cannavo et al. (2008) and Ranatunga et al. (2008), a large proportion of crop nitrogen models (7 out of 16) and soil water models (13 out of 21) that have been widely applied in Australia employ the cascade approaches for soil water dynamics. Such models also include the newly developed AquaCrop model for irrigation scheduling developed by the FAO (Steduto et al., 2009; Raes et al., 2009). Although the cascade approaches are simple and easy to implement, they do not satisfactorily simulate soil water movement at daily intervals (Gandolfi et al., 2006), and so are less accurate in estimating evaporation and water uptake by crops.

Over the last few decades not only has the basic theory of water movement in soil, i.e. the Richards' equation, become generally accepted, but the modeling of soil water dynamics has progressed significantly through advances in mathematics and computer science. The numerical schemes such as the finite element method used for the solution to the basic equation are well developed (Šimůnek et al., 2008), and software such as HYDRUS is readily available for 1-D or multi-dimensional simulations (Šimůnek et al., 2005; 2006). In the simulations of soil water dynamics in the soil-crop system, the models using the basic equation such as the SWAP model developed by Kroes et al. (2008) have also developed. A new simple and explicit algorithm for the basic equation has recently been proposed (Yang et al., 2009). Despite the progress made, the take-up of such theory based flow models for the practical uses is still low, largely because of difficulties in making satisfactory estimates of soil hydraulic properties at a field scale (Bastiaanssen et al., 2007). It is, therefore, important to devise reliable methods for estimating soil water properties for use in such flow based models.

There are a number of ways to determine the soil hydraulic properties, including: direct measurements (Van Genuchten et al., 1991); estimation using pedo-transfer functions (PTFs) (Wösten et al., 1999; Hwang and Powers, 2003; Cresswell et al., 2006); and inverse modeling techniques (Hopmans and Šimunek, 1999). Direct measurements are usually carried out under laboratory conditions, but they are time consuming and require complex measuring devices. Further, the measurements are made on small cores, suffering from the edge effects caused by water movement at the soil-container interface. PTFs methods, on the other hand, are based on soil texture and particle-size distribution data, and are easy to use. However, there are inconsistencies in the derived soil hydraulic properties between different models (Hwang and Powers, 2003).

The third approach is to deduce the soil characteristics using inverse modeling techniques. Such techniques have proven promising to estimate the parameters required by physically based agro-hydrological models (Bastiaanssen et al., 2007), and have received enormous efforts in the last couple of decades. While many scientists (Nützmann et al., 1998; Finsterle and Faybishenko, 1999; Bohne and Salzmann, 2002; Bitterlich et al., 2004; Minasny and Field, 2005; Schmitz et al.,

2005) used the measured soil water content and soil pressure head data on small cores under laboratory conditions, which still suffers from the edge effects, others (Jhorar et al., 2002; Ines and Droogers, 2002; Sonnleitner et al., 2003; Ritter et al., 2003) attempted to infer soil hydraulic parameters from simulation models using data for cropped soils gathered in the field. However, the interpretation of data from cropped soils is strongly dependent on the way in which the selected model quantifies the root density distribution in the profile and the relationship between root water uptake and soil water availability. Due to the uncertainty of root density distribution and the lack of consistency between the results from two types of model, i.e. uptake without water stress compensation (Feddes et al., 1978; Šimunek et al., 1992) and with compensation (Li et al., 2001, 2006), questions are raised about the robustness of the deduced soil hydraulic properties. This suggests that a more reliable approach would be to use data from uncropped soils for the inverse analysis. Gómez et al. (2009) succeeded to identify the soil hydraulic conductivity by applying an inverse technique on data from a field drainage experiment. However, the work is unable to be directly applied for the water dynamics in the soil-crop system because of the lack of the relationship between soil water content and soil pressure head. In the area of developing new optimization algorithms for inferring soil hydraulic properties, research has also been active and fruitful (Huyer and Neumaier, 1999; Abbaspour et al., 2001; Schmitz et al., 2005).

The principles behind estimating soil hydrulic parameters using an inverse modeling technique involve three different steps: determining the number of identified parameters, formulating the optimized function, and implementing an optimization algorithm. In general, the identified parameter number should be kept to the minimum. Thus, if the parameters can be determined with certainty in advance, they should be treated as known parameters. The selection of an effective optimization algorithm is important for solving the inverse problem. Although there are many traditional algorithms available (Rao, 1984; Hopmans and Šimunek, 1999), they are only able to find a localized optimum solution which is highly dependent on the initial estimates of the optimized parameters. Such algorithms are not directly applicable to the problem in this study. New algorithms have been proposed which facilitate a global search. These include evolutionary Genetic Algorithms (GAs) based on a natural selection rule (Holland, 1975; Goldberg, 1989; Carroll, 1999). The algorithm has been successfully applied in identifying soil water hydraulic properties (Ines and Droogers, 2002).

Hopmans and Šimunek (1999) and Romano and Santini (1999) have stressed that careful consideration must be given to the construction of the optimized function, so that the inverse problem is properly posed. Whether it is successful in solving the inverse problem is largely dependent on how the optimized function is constructed. It has been widely reported to use soil water content data in the formulation of the optimized function. For example, Bohne and Salzmann (2002) and Ritter et al. (2003) used the mean squared residuals of soil water content between the measured and simulated data in the optimized function. To improve the identifiability of the inverse problem, the inclusion of information other than soil water content such as evapotranspiration has also been attempted (Ines and Droogers, 2002). However, the construction of such an optimized function was made possible only when the actual evapotranspiration was directly measured. In the field experiments, the measurement of actual evapotranspiration is difficult. Therefore, the incorporation of additional soil characteristic information which can be easily measured in the optimized function should be sought to make the inverse problem better posed, and thus to increase the identifiability of the inverse problem and the uniqueness of the identified parameters.

The objective of the study was therefore to evaluate the use of a new optimized function and an inverse simulation approach using a GA technique for estimating soil hydraulic properties at a field scale. The new function was, for the first time, constructed from dynamic water distribution data down the soil profile from a 'calibration' experiment in a fallow soil, and the soil water at field capacity. The reliability of the inferred soil water properties was then examined in predicting soil water dynamics in an independent 'verification' experiment carried out on a leek crop on the same site.

2. Experiments

Two experiments were carried out, both on a sandy loam of the Wick series (Whitfield, 1974) in Big Ground field at Wellesbourne, UK. One is used to deduce soil hydraulic properties from soil water contents at various depths under bare fallow conditions over time collected from an evaporation experiment (calibration experiment). The other is used to provide independent data for testing the validity of the inferred soil hydraulic properties by simulating water dynamics using a plant-soil model (verification experiment).

The calibration experiment was conducted from 27 April (Day 117) to 21 November (Day 325) in 1971 (Burns, 1974). Physical properties of this soil are given in Table 1 (after Burns, 1974). The profile consisted of fairly uniform soil to a depth of 25 cm and a slight increase in the sand content to the measured depth of 45 cm, with no significant cracks in the profile. Soil samples from 4 replicate plots were taken at 5 cm increments to a depth of 45 cm (using a 2.54 cm internal diameter soil tube) at regular intervals throughout the experiment. Five cores were taken at random from each plot and the corresponding depth increments combined. Soil water contents in the samples were measured by drying at 105ºC for 24 h. In total 9 measurements of soil water content down the profile on Day 118, 131, 168, 189, 204, 229, 250, 278 and 319 were taken during the experiment. Corresponding measurements of field capacity for the same soil were made on three replicate plots after applying excess irrigation and covering the soil with polythene sheeting for 48 h to prevent evaporation (Burns, 1974). Daily values of rainfall and the climatic variables of minimum, mean and maximum air temperatures were recorded at the on-site weather station within 400 m of the experimental site.

The verification experiment was carried out in the same area of the same field from 15 April (Day 105) to 15 October (Day 284) 1973. The soil was cropped with leek (var. The Lyon), and was direct drilled at a row spacing of 55 cm on 15 April. The experiment was arranged in a randomized block design with 3 replicate plots (each 10 m x 1 m). All fertilizer, herbicide and pesticide applications were made according to conventional practice. No irrigation was applied to the plots once the crop was established. Two measurements of the distribution of roots, nitrogen, potassium, phosphate and soil water were made on 08 August (Day 220) and 03 September (Day 246) 1973. Soil samples were taken on each date using a pinboard (with 5 cm pins arranged in a 5 cm by 5 cm matrix) which was driven into the vertical side of a newly dug pit located across a selected crop row (Goodman and Burns, 1975). On each occasion the board was positioned to take soil samples across the whole plant row (between the midpoints of successive rows) to a depth of 45 cm. It was then dug out of the soil, trimmed, and individual 5 x 5 x 5 cm samples removed for lab analysis. The measured root distribution and soil water related data was used in the current study to test the reliability of the reduced soil hydraulic properties. Daily measurements of the climatic variables were made at the on-site weather station as for the calibration experiment.

3. Theory

3.1. Description of the flow model

3.1.1. Soil water flow

In a 1-D situation, the Richards equation governing water flow in an isotropic variably saturated soil with a sink term is (Celia et al., 1990; Šimunek et al., 1992):

$$\frac{\partial \theta}{\partial t} = \frac{\partial}{\partial z}[K(\frac{\partial h}{\partial z} - 1)] - S(z) \quad (1)$$

where t (d) is time, z (cm) is the vertical coordinate, K (cm d^{-1}) is the soil hydraulic conductivity, h (cm) is the soil pressure head, and S (cm d^{-1}) is the sink term, representing the volume of water extracted from a soil unit.

The soil hydraulic functions are defined according to van Genuchten (1980) and Mualem (1976):

$$\Theta = \frac{\theta - \theta_r}{\theta_s - \theta_r} = [\frac{1}{1+|\alpha h|^n}]^m \qquad (2)$$

$$K(h) = K_s \Theta^{0.5} [1-(1-\Theta^{1/m})^m]^2 \qquad (3)$$

where Θ is the relative saturation, θ_s and θ_r (cm^3 cm^{-3}) are the saturated and residual soil water contents, α (cm^{-1}) and n are the shape parameters of the retention and conductivity functions, m=1-1/n, K_s (cm d^{-1}) is the saturated hydraulic conductivity.

3.1.2. Soil evaporation and crop transpiration

Daily potential crop evapotranspiration is calculated using a FAO 56 crop coefficient method (Allen et al., 1998):

$$ET_c = K_c ET_0 \qquad (4)$$

where ET_c (mm d^{-1}) is the daily potential evapotranspiration, K_c is the crop coefficient and ET_0 (mm d^{-1}) is the reference evapotranspiration, which is estimated directly at daily intervals using a Hargreaves method recommended by the FAO when the Penman-Monteith method cannot be applied due to lack of measured climatic information (Allen et al., 1998):

$$ET_0 = 0.000938\ R_a (T + 17.8)(T_{max} - T_{min})^{0.5} \quad (5)$$

where T_{min}, T and T_{max} (°C) are the minimum, mean and maximum air temperature, and R_a (MJ m^{-2} d^{-1}) is the total incoming extraterrestrial solar radiation which is expressed as (Allen et al, 1998):

$$R_a = \frac{24 \times 60}{\pi} \times 0.082 d_r [\omega_s \sin(\varphi)\sin(\delta) + \cos(\varphi)\cos(\delta)\sin(\omega_s)] \quad (6)$$

in which

$$d_r = 1 + 0.033\cos(\frac{2\pi}{365} J) \quad (7)$$

$$\delta = 0.409\sin(\frac{2\pi}{365} J - 1.39) \quad (8)$$

$$\omega_s = \arccos[-\tan(\varphi)\tan(\delta)] \quad (9)$$

where d_r is the relative distance between the earth and the sun, J is the day number in the year, δ (radian) is the solar declination, φ (radian) is the latitude, and ω_s is the sunset hour angle.

The crop coefficient method partitions the K_c factor into two separate coefficients:

$$K_c = K_{cb} + K_e \quad (10)$$

where K_{cb} is the basal crop coefficient for transpiration, and K_e is the evaporation coefficient. K_{cb} depends on crop species and its development stage.

For the evaporation coefficient, K_e is defined as:

$$K_e = \min(K_{c\max} - K_{cb}, fK_{c\max}) \tag{11}$$

where K_{cmax} is the maximum evapotranspiration coefficient, and f is the soil fraction not covered by plants and exposed to evaporation as described by Allen et al. (1998).

3.1.3. Root water uptake

The rate of root water uptake, expressed as in Feddes et al. (1978) and Wu et al. (1999), is:

$$S(z) = \alpha(h)S_{\max}(z,h) \tag{12}$$

where α is the root water stress reduction factor, and S_{max} (cm d^{-1}) is the maximum root water uptake rate.

In the calculation of maximum root water uptake it is assumed that all roots have identical physical properties, and therefore have uniform water uptake capacity regardless their age or location. The water uptake rate from the different parts of the root zone is dependent on root density. By assigning the potential transpiration to the root zone, the maximum root water uptake rate can be calculated as follows:

$$S_{\max}(z) = \frac{l(z) K_{cb} ET_0}{\int_z l(z) dz} \quad (13)$$

where $l(z)$ is the root density distribution down the profile.

The reduction of transpiration is caused by the decline in water uptake by the roots in the dry parts of the soil. Following Feddes et al. (1978), Šimunek et al. (1992), Wu et al. (1999) and Sonnleitner et al. (2003), root water uptake is assumed to be zero when soil pressure head is below h_3, i.e. the soil pressure head at the permanent wilting point (h_3 = -15000 cm), and is unlimited for soil pressure head between h_1 and h_2^{high} for a rapid transpiration and h_2^{low} for a slow transpiration. The increase in water uptake between h_3 and h_2 is linearly related to the soil pressure head. Water uptake is also assumed to be 0 at saturation due to lack of oxygen in the root zone, i. e.

$$\alpha(h) = \begin{cases} 0 & h \le h_3 \\ (h - h_3)/(h_2 - h_3) & h_3 < h < h_2 \\ 1 & h_2 \le h < h_1 \\ h / h_1 & h \ge h_1 \end{cases} \quad (14)$$

The actual transpiration rate T_{act} (cm d^{-1}) is therefore calculated:

$$T_{act} = \int_z S(z) dz \quad (15)$$

3.2. Inverse analysis model

Estimating soil water parameters using an inverse modeling technique includes the determination of the number of identified parameters, the formulation of the optimized function and the implementation of an optimization algorithm.

3.2.1. Identified parameters

There are five soil hydraulic parameters in the van Genuchten equation (Eqs. 2 and 3). Attempts have been made to use fewer soil hydraulic parameters by fixing known or insensitive parameters which can be estimated with certainty to enhance the uniqueness of the inversely analyzed solution. Jhorar et al. (2002) fixed θ_r and K_s when implementing an optimization algorithm to the inverse problem as sensitivity analyses of parameters revealed that they were insensitive to the model's response. This was also found to be the case for the calibration experiment in this study. Sensitivity analyses show that θ_r, K_s and α are much less sensitive than θ_s and n to the mean squared residuals of soil water contents obtained at different depths and intervals between measurement and simulation (Fig. 1). The analyses were carried out using the soil hydraulic properties derived from PTFs proposed by Wösten et al. (1999), i. e. $[\theta_s, \theta_r, \alpha, n, K_s]^T$ =[0.336, 0.025, 1.218, 0.04869, 28.88]^T, together with other parameter values explained in the following section. Ritter et al. (2003), on the other hand, set a value for soil water content at saturation in advance. However, none of the above parameters were measured or could be determined with certainty in our study. We therefore used the whole set of the van Genuchten parameters in the inverse analysis.

3.2.2. Formulation of the optimized function

In the formulation of an optimized function, we used two criteria in this study, i.e. soil water content θ, θ and soil water content at field capacity θ_{FC}. The primary reason of including θ_{FC} was that the experiments for measuring θ_{FC} were carried out under field conditions, and the measured value was considered more representative for the soil at the field scale.

To solve the optimization problem, a Genetic Algorithm (GA) technique was adopted. Two fitness functions containing θ (Eq. 16), and θ and θ_{FC} (Eq. 17) were tested. Since the measured soil water content at field capacity was representative for the soil at the field capacity, a much bigger weight was assigned to θ_{FC} than θ in Eq. (17) to ensure that the inferred soil water content at field capacity was close to the measured value.

$$\text{Max. } f_1(\mathbf{x}) = -\frac{1}{N}\sum_{i=1}^{N}[\theta_{mea}(t_i) - \theta_{sim}(t_i, \mathbf{x})]^2 \quad (16)$$

$$\text{Max. } f_2(\mathbf{x}) = -\{\frac{1}{N}\sum_{i=1}^{N}[\theta_{mea}(t_i) - \theta_{sim}(t_i, \mathbf{x})]^2 + (\theta_{FC,mea} - \theta_{FC,sim})^2\} \quad (17)$$

where f_1 and f_2 are the fitness functions, **x** is the parameter vector, i.e van Genuchten soil water parameters, θ_{mea} and θ_{sim} (i.e. θ in the flow equation) are the measured and simulated soil water content at depths in the profile, t_i (d) is the time when the i^{th} measurement is taken, N is the number of measurements, and $\theta_{FC,mea}$ and $\theta_{FC,sim}$ are the measured and simulated soil water content at field capacity, respectively. To determine $\theta_{FC,mea}$ excess irrigation was first applied and the soil was covered with polythene sheeting for 48 h to prevent evaporation. The soil samples were then taken from three replicate plots and soil water contents were measured (Burns, 1974). $\theta_{FC,sim}$ was defined as the soil water content at the soil pressure head of -330 cm.

3.2.3. Optimization algorithm

GAs are global search heuristics to find exact or approximate solutions to optimization and search problems based on the evolutionary ideas of natural selection. They are implemented in a computer simulation in which a population of abstract representations of candidate solutions to an optimization problem evolves toward better solutions. The evolution starts from a population of randomly generated individuals and happens in generations. In each generation, the fitness function of every individual in the population is evaluated, multiple individuals are stochastically selected from the current population (based on their fitness), and modified to form a new population through genetic operators of crossover (recombination) and mutation. For each new solution to be produced, a pair of "parent" solutions is selected for breeding from the pool. A new solution shares many of the characteristics of its "parents". New parents are selected for each new child, and the process continues until a new population of solutions of appropriate size is generated. The new population is then used in the next iteration of the algorithm. The algorithm terminates when a termination condition has been reached, commonly a maximum number of generations has been produced. Detailed procedure of implementing a GA is given in Goldberg (1989).

The technique and corresponding software used in the study was a micro-GA, developed by Carroll (1999). The advantage of using this technique is that the software not only includes many GA concepts, such as creep mutation and uniform crossover, but is also very effective. Compared to a conventional GA, which normally requires a large population size and a large number of generations, the adopted micro-GA performs excellently for a small population size. For many cases a population of as few as 5 can achieve satisfactory results within 100 generations (Carroll, 1999).

Soil hydraulic parameters were inferred from all measured soil water contents at different depths and intervals in a fallow field subject to natural rainfall and evaporation in the calibration experiment. The reliability of the deduced soil water parameters was tested in reproducing data of soil water content collected from the verification experiment on the same soil cropped with leek.

3.3. Evaluation criteria

Accuracy of the simulated soil water content using deduced parameters was evaluated using the model efficiency coefficient (EF) (Nash and Sutcliffe, 1970), the root of the mean squared errors (RMSE) and the mean absolute error (MAE) (Bohne and Salzmann, 2002; Ritter et al., 2003; Merdun et al., 2006):

$$EF = 1 - \frac{\sum_{i=1}^{N} [\theta_{mea}(t_i) - \theta_{sim}(t_i, \mathbf{x})]^2}{\sum_{i=1}^{N} [\theta_{mea}(t_i) - \overline{\theta_{mea}(t_i)}]^2} \qquad (18)$$

$$RMSE = \sqrt{\frac{1}{N}\sum_{i=1}^{N}[\theta_{mea}(t_i) - \theta_{sim}(t_i, \mathbf{x})]^2} \quad (19)$$

$$MAE = \frac{1}{N}\sum_{i=1}^{N}|\theta_{mea}(t_i) - \theta_{sim}(t_i, \mathbf{x})| \quad (20)$$

where $\overline{\theta_{mea}}$ is the average of the measured values.

An efficiency of 1 ($EF = 1$) corresponds to a perfect match of simulated and measured data. A small *RMSE* and *MAE* indicate that the simulated values are in good agreement with the measured values.

4. Parameter values

4.1. The calibration case

The inverse modeling procedures were implemented on data of measured soil water content from the calibration experiment. As the soil is fairly uniform throughout its profile, it was characterized by depth-independent values of the parameters θ_s, θ_r, α, n and K_s. In the forward simulation, the first measured data of soil water content down the profile (Day 118) were taken as the initial condition. The measured daily rainfall and the potential evaporation, calculated using the FAO approach (Allen et al., 1998), were used as inputs (Fig. 2). Daily rainfall and evaporation were assumed to be uniformly distributed throughout the day. Simulated water contents were to 42.5 cm, the deepest depth at which measurements from the calibration experiment were made.

Since boundary conditions have a great effect on the accuracy of simulation (Boone and Wetzel, 1996; Lee and Abriola, 1999), we used measured soil water contents at the deepest depth for the condition at the lower boundary. The maximum water influx from the soil surface was the difference between rainfall and evaporation. The actual evaporation, however, was often less than the maximum because the surface soil was not wet enough to permit a sufficient water flux to meet potential demand. The rate of water transport depends critically on the soil wetness near the surface. The soil flow equation was solved using a Galerkin type linear finite element scheme (Šimunek et al., 1992). The soil domain was divided into 32 soil layers with thin layers in the top and the bottom where the upper and lower boundary conditions were imposed. The thickness of soil layers ranged from 0.2 cm to 2 cm. The lower and upper values for the 5 parameters were set as: θ_s (0.3-0.5), θ_r (0.001-0.1), α (0.01-0.2), n (1.05-1.8), and K_s (10.0-250.0), wide enough to describe the soil in this study. We implemented the optimization procedures to the fitness functions Eq. (16) and Eq. (17). The population size was set to 5 as suggested by Carroll (1999). However, in order to study the effect of the population size on the parameter estimation, we also used a population of 10 in the optimization procedures.

4.2. The verification case

The reliability of the deduced soil water parameters was tested against data of soil water content collected from the verification experiment on 08 August (Day 220) and 03 September 1973 (Day 246) on the same soil cropped with leek. The parameters h_1, h_2^{high} and h_2^{low} were set to be -1 cm, -500 cm and -1100 cm as suggested by Šimunek et al. (1992) and Sonnleitner et al. (2003). The potential crop evapotranspiration during the period was estimated using the FAO approach (Allen et al., 1998). In the calculation, the values of 1.35 and 0.9 were used for the parameters of K_{cmax} and K_{cb} (Allen et al., 1998). No significant rainfall events occurred in the period (Fig. 3). The simulation began from 08 August 1973, and the observed distribution of soil water content on that day was used as the initial condition. The calculated soil depth was 45 cm and the lower boundary condition was set as free drainage, as in Rowse et al. (1978) who simulated soil water movement on the same cropped soil. This was a fairly accurate representation of the field conditions according to their measurements.

5. Results and discussion

5.1. Deduction of soil water parameters from the calibration experiment

The deduced values of the parameters based on the fitness function Eq. (16) show that the simulated results were slightly better with the population of 10 than 5 in terms of *RMSE* and *EF*, while opposite is the case in terms of *MAE* (Table 2). Based on the fact that in both cases the results of *RMSE*, *MAE* and *EF* are all extremely close to each other, it is difficult to decide which population size is better. However, the deduced values of the parameters were rather different. For example, the deduced θ_s of 0.332 with the population of 5 was much less than the value of 0.422 inferred with the population of 10. This indicates that the proposed criteria solely based on soil water content (Eq. 16) yielded different sets of parameter values with very similar model responses, i.e. the inverse solution was not unique. This non-uniqueness phenomenon is commonly faced and reported in the literature (Hopmans and Šimunek, 1999). The major reason for such a phenomenon is that the problem is highly non-linear, and the fitness function is not well posed. It can also be partly attributed to lack of measurements at the wet end of the soil water retention curve. In the study there were few measurements of soil water content above or near to the field capacity.

The non-uniqueness solution to the inverse problem was effectively overcome by adopting the hybrid fitness function Eq. (17). Results reveal the soil water retention curves inferred from different population sizes agree with each other well, indicating that the hybrid fitness function (Eq. 17) was better posed than Eq. (16) (Fig. 4). The calculated values for the evaluation criteria *RMSE* and *MAE* were satisfactory, and the *EF* value was fair (Table 2). To compare the inferred soil hydraulic properties with those derived from other alternative approaches, retention curves derived from PTFs proposed by Wösten et al. (1999) and Cresswell et al. (2006) were also calculated (Fig. 4). It was assumed that soil water content at saturation from Cresswell et al. (2006) was the same as that from Wösten et al. (1999), since Cresswell et al's approach did not offer a solution to estimating the saturated soil water content. The functions proposed by Wösten et al. (1999) were based on a study of more than 5000 soil samples across Europe. Both PTFs derived retention curves are close to each other and the corresponding volumetric water contents over a wide range of given pressure heads were about 0.07 to 0.1 cm^{-3} cm^{-3} less than those calculated from GA.

Overall comparison of soil water content between measurement and simulation (Fig. 5) and the detailed comparisons were made between simulated and measured soil water contents down the soil profile measured at intervals in the calibration experiment (Fig. 6). The simulated water contents were calculated from the flow model using the deduced parameter values (Table 2) for a population size of 10 with a hybrid fitness function (Eq. 17). The simulated values of soil water content are in good agreement with the measured values, and the values of *RMSE* (0.024 cm^3 cm^{-3}) and *MAE* (0.0194 cm^3 cm^{-3}) are small. Over the 64 comparisons only 5 differed by more than 0.04 cm^3 cm^{-3} and the biggest difference was 0.085 cm^3 cm^{-3}. The overall agreement between measurement and simulation is fairly good, which is illustrated in Fig. 5 where the measurements against simulated values are all close to the 1:1 line. The detectable discrepancies between simulated and measured values were mainly near the top and the middle of the profile (Fig. 6). The measured values near the surface tended to be lower than the simulated ones, while in the middle, the opposite appears to be the case. This may be explained by the heterogeneity of soil in the profile, with the profile having a lower field capacity at the top and a relatively larger one in the middle (Table 1). In the process of inverse modeling, we assumed the soil was homogenous throughout the profile.

The cumulative rainfall, potential and actual evaporation during the experiment are shown in Fig. 7. It reveals that the actual evaporation is considerably less than the potential one. By the end of the experiment the cumulative actual evaporation was 27 cm, only about 40% of the cumulative potential value. This might be attributed to the dryness of the soil in the top 5 cm layer during the most of the experiment period (Fig. 8a). Except for the three periods between Day 160 to 172, Day 205 to 230 and Day 285 to 295 which coincided with major rainfall events (Fig. 2), soil water content in the top 5 cm layer was low, close to 0.2 cm^3 cm^{-3} (Fig. 8a), resulting in reduction in evaporation. Another contributory factor is that the potential evaporation might be over-estimated by the Hargreaves method simply based on the air temperatures used in the study. The cumulative actual evaporation was also less than cumulative rainfall, which was partly caused by drainage at the lower boundary of the soil profile, particularly in the three periods when rainfall clearly exceeded the evaporation demand (Fig. 8b).

5.2. Simulation of water dynamics in the soil-crop system in the verification experiment

Relative root density distributions were measured using a pin board technique (Goodman and Burns, 1975) on 08 August (Day 220) and 03 September (Day 246) 1973 and averaged (Fig. 9a). The rooting depth was 27.5 cm, and the maximum root density occurred at 8 cm below the soil surface. Such a pattern of root distribution where the maximum root density is found some distance from the soil surface rather than the top is in accordance with measurements from other vegetable crops such as cabbage, carrot and lettuce (Thorup-Kristensen, 2006). As previous studies (Gerwitz and Page, 1974; Pedersen et al., 2009) have also shown that the root density declines down the soil profile in an approximately exponential manner, we derived the following equation to describe the relative root density by fitting an exponential equation to the measured data in the analysis:

$$l(z) = \begin{cases} e^{-0.11(z - z_{r\max})} & z_{r\max} \le z < 0 \\ e^{0.11(z - z_{r\max})} & z < z_{r\max} \end{cases} \quad R^2 = 0.979 \qquad (21)$$

where z_{rmax} (= -8 cm) is the vertical coordinate where the maximum root density occurs. Good agreement of relative root density distribution between measured and modeled with Eq. (21) was observed (Fig. 9a).

Simulated and measured soil water content in the profile on 03 September 1973 was compared (Fig. 9b). Apart from a marked discrepancy in the top 5 cm region, the simulated water content not only reproduced the measured pattern, but also agreed with the measured data well (with the maximum error of less than 7%). The discrepancy in the near surface region may partly be attributed to the simplified assumption that the soil was homogenous throughout the profile even though the soil near the surface had a lower ability to retain water (Table 1) as explained earlier. The soil water content in the root zone was close to the permanent wilting point, indicating that the plants were under severe water stress at the later stages of the simulation period.

Root water uptake from different 5 cm soil layers were simulated according to Eq. (12) (Fig. 10a). Since there were no rainfall events in the early stages of the simulation, roots depleted the soil water rapidly in the top soil layers. Under the dual action of evaporation and transpiration, the top 5 cm soil layer dried out with no water uptake possible in the first 3 days as the soil water content rapidly dropped to the permanent wilting point of 0.16 cm^3 cm^{-3} (Fig. 10b). After 7 days, the drought spread to the 20 cm soil depth. The water contents in the soil layers between 5 to 20 cm were all close to the permanent wilting point, while the water content in the top 5 cm layer was even lower due to evaporation (Fig. 10b). The plants suffered from severe water stress between Day 227 to Day 238 when only water below 20 cm was available for root uptake. The sudden increase in water uptake from the top layer was caused by rainfall on Day 238 (Fig. 10a). Rain water did not penetrate to the second layer as the noticeable change in water content was restricted to the top 5 cm layer (Fig. 10b). Only from below 20 cm was water constantly available for uptake. This is a result of low root demand and of capillary flow from lower soil layers.

6. Conclusions

Soil hydraulic properties were accurately deduced from soil water contents measured at intervals down a fallow field soil by setting up a new optimized function and optimizing it with a micro-GA optimization tool. It supports the view that micro-GA provides a powerful means of searching for a global optimum. The new optimized function constructed using both soil water content and soil water at field capacity is better than that using solely soil water content to overcome the problem of non-unique parameter estimation in inverse modeling. The latter were exacerbated by the lack of measurements at the wet end of the soil water retention curve. To improve the uniqueness of the identified parameters, special attention needs to be given to collecting soil water data when the soil is wet in a field evaporation experiment.

Results from the study also confirm that an exponential function can accurately describe root distribution down the soil profile with the maximum root density of leek found 8 cm below the soil surface. Good predictions of soil water content in the cropped soil indicate that the approach employed for the deduction of the effective soil hydraulic properties is effective, and the way of simulating water dynamics in the soil-crop system using the FAO dual crop coefficient method for estimating potential evaporation and transpiration is reasonable.

Acknowledgements

The work was partly supported by the UK Department for Environment, Food and Rural Affairs in projects HH3507SFV and HH3509SFV.

References

Abbaspour, K.C., Schulin, R., van Genuchten, M.Th., 2001. Estimating unsaturated soil hydraulic parametersusing ant colony optimization. Adv. Water Resour. 24, 827-841.

Allen, R.G., Pereira, L.S., Raes, D., Smith, M., 1998. Crop evapotranspiration. Guidelines for computing crop water requirements. FAO Irrigation and Drainage Paper 56. FAO, Rome.

Bastiaanssen, W.G.M., Allen, R.G., Droogers, P., D'Urso, G., Steduto, P., 2007. Twenty-five years modeling irrigated and drained soils: State of the art. Agric. Water Manage. 34, 137–148.

Bitterlich, S., Durner, W., Iden, S.C., Knabner, P., 2004. Inverse estimation of the unsaturated soil hydraulic properties from column outflow experiments using free-form parameterization. Vadose Zone J. 3, 971-981.

Bohne, K., Salzmann, W., 2002. Inverse simulation of non-steady-state evaporation using nonequilibrium water retention data: a case study. Geoderma 110, 49-62.

Boone, A., Wetzel, P.J., 1996. Issues related to low resolution modeling of soil moisture: Experience with the PLACE model. Global Planet. Change 13, 161-181.

Burns, I.G., 1974. A model for predicting the distribution of salts applied to fallow soils after excess rainfall for evaporation. J. Soil Sci. 25, 165-178.

Cannavo, P., Recous, S., Parnaudeau, V., Reau, R., 2008. Modelling N dynamics to assess environmental impacts of cropped soils. Adv. Agron. 97, 131-174.

Carroll, D.L., 1999. http://cuaerospace.com/carroll/ga.html.

Celia, M.A., Bouloutas, E.T., Zarba, R.L., 1990. A general mass-conservative numerical solution for the unsaturated flow equation. Water Resour. Res. 26, 1483-1496.

Cresswell, H.P., Coquet, Y., Bruand, A., McKenzie, N.J., 2006. The transferability of Australian pedotransfer functions for predicting water retention characteristics of French soils. Soil Use Manage. 22, 62-70.

Droogers, P., Tobari, M., Akbari, M., Pazira, E., 2001. Field-scale modeling to explore salinity problems in irrigated agriculture. Irrig. Drain. 50, 77-90.

Feddes, R.A., Kowalik, P.J., Zaradny, H., 1978. Water uptake by plant roots. In: Feddes, R.A., Kowalik, P.J., Zaradny, H. (Eds.), Simulation of Field Water Use and Crop Yield. John Wiley & Sons, Inc., New York, pp. 16-30.

Finsterle, S., Faybishenko, B., 1999. Inverse modeling of a radial multistep outflow experiment for determining unsaturated hydraulic properties. Adv. Water Resour. 22, 431-444.

Gandolfi, C, Facchi, A., Maggi, D., 2006. Comparison of 1D models of water flow in unsaturated soils. Environ. Modell. Softw 21, 1759-1764.

Gerwitz, A., Page, E.R., 1974. Empirical mathematical - model to describe plant root systems 1. J. Appl. Ecol. 11, 773-781.

Goldberg, D.E., 1989. Genetic Algorithms in Search, Optimization and Machine Learning. Addison-Wesley, Reading, Mass.

Gómez, S., Severino, G., Randazzo, L., Toraldo, G., Otero, J.M., 2009. Identification of the hydraulic conductivity using a global optimization method. Agric. Water Manage. 96, 504-510.

Goodman, D., Burns, I.G., 1975. Nutrient distribution in a cropped soil. Rep. Natn. Veg. Res. Stn for 1974, The British Society for the promotion of vegetable research Wellesbourne UK, p. 49.

Holland, J.H., 1975. Adaptation in Natural and Artificial Systems. University of Michigan Press.

Hopmans, J.H., Šimunek, J., 1999. Review of inverse estimation of soil hydraulic properties. In: Van Genuchten, M.Th., Leij, F.J., Wu, L. (Eds.), Characterization and Measurement of the Hydraulic Properties of Unsaturated Porous Media. University of California, CA, pp. 634-659.

Huyer, W., Neumaier, A., 1999. Global optimization by multilevel coordinator search. J. Global Optim.14, 331-355.

Hwang, S.II., Powers, S.E., 2003. Using particle-size distribution models to estimate soil hydraulic properties. Soil Sci. Soc. Am. J. 67, 1103-1112.

Ines, A.V.M., Droogers, P., 2002. Inverse modeling in estimating soil hydraulic functions: a Genetic Algorithm approach. Hydrol. Earth Syst. Sci. 6, 49-65.

Jhorar, R.K., Bastiaanssen, W.G.M., Feddes, R.A., Van Dam, J.C., 2002. Inversely estimating soil hydraulic functions using evapotranspiration fluxes. J. Hydrol. 258, 198-213.

Kroes, J.G., Van Dam J.C., Groenendijk P., Hendriks R.F.A., Jacobs C.M.J., 2008. SWAP version 3.2. Theory description and user manual. Wageningen, Alterra, Alterra Report1649, 262 pp.

Lee, D.H., Abriola, L.M., 1999. Use of the Richards equation in land surface parameterization. J. Geophys. Res. 104, 27519-27526.

Li, K.L., Jong, R.De, Boisvert, J.B., 2001. An exponential root-water-uptake model with water stress compensation. J. Hydrol. 252, 189–204.

Li, K.Y., Jong, R.De, Coe, M.T., Ramankutty, N., 2006. Root-water-uptake based upon a new water stress reduction and an asymptotic root distribution function. Earth Interac.10, 1-22.

Merdum, H., Cinar, O., Meral, R., Apan, M., 2006. Comparison of artificial neural network and regression pedotransfer functions for prediction of soil water retention and saturated hydraulic conductivity. Soil Till. Res. 90, 108-116.

Minasny, B., Field, D.J., 2005. Estimating soil hydraulic properties and their uncertainty: the use of stochastic simulation in the inverse modelling of the evaporation method. Geoderma 126, 277-290.

Mualem, Y., 1976. A new model for predicting the hydraulic conductivity of unsaturated porous media. Water Resour. Res. 12, 513-522.

Nash, J.E., Sutcliffe J.V., 1970. River flow forecasting through conceptual models part I — A discussion of principles. J. Hydrol. 10, 282–290.

Nützmann, G., Thiele, M., Maciejewski, S., Joswig, K., 1998. Inverse modelling techniques for determining hydraulic properties of coarse-textured porous media by transient outflow methods. Adv. Water Resour. 22, 273-284.

Pedersen, A., Zhang, K., Thorup-Kristensen, K., Jensen, L.S., 2009. Modelling diverse root density dynamics and deep nitrogen uptake – A simple approach. Plant Soil. DOI: 10.1007/s11104-009-0028-8.

Raes, D., Steduto, P., Hsiao, T.C., Fereres, E., 2009. AquaCrop - The FAO crop model to simulate yield response to water: II. Main algorithms and software description. Agron. J. 101, 438-447.

Rahn, C.R., Zhang, K., Lillywhite, R., Ramos, C., Doltra, J., de Paz, J.M., Riley, H., Fink, M., Nendel, C., Thorup-Kristensen, K., Pedersen, A., Piro, F., Venezia, A., Firth, C., Schmutz, U., Rayns, F., Strohmeyer, K., 2009. EU-Rotate_N – a

European decision support system – to predict environmental and economic consequences of the management of nitrogen fertiliser in crop rotations. Eur. J. Horti. Sci. In press.

Rao, S.S., 1984. Optimization: Theory and Application. Wiley Eastern Limited.

Renaud, F.G., Bellamy, P.H., Brown, C.D., 2008. Simulating pesticides in ditches to assess elological risk (SPIDER): I. Model description. Sci. Total Environ. 394, 112-123.

Ritchie, J.T., 1998. Soil water balance and plant water stress. In: Tsuji, G.Y. (Ed), Understanding Options for Agricultural Production, pp. 41-54.

Ritter, A., Hupet, F., Munoz-Carpena, R., Lambot, S., Vanclooster, M., 2003. Using inverse methods for estimating soil hydraulic properties from field data as an alternative to direct methods. Agric. Water Manage. 59, 77-96.

Ranatunga, K., Nation, E.R., Barratt, D.G., 2008. Review of soil water models and their applications in Australia. Environ. Modell. Softw. 23, 1182-1206.

Romano, N., Santini, A., 1999. Determining of soil hydraulic functions from evaporation experiments by a parameter estimation approach: experimental verifications and numerical studies. Water Resour. Res. 35, 3343-3359.

Rowse, H.R., Stone, D.A., Gerwitz, A., 1978. Simulation of the water distribution in soil II. The model cropped soil and its comparison with experiment. Plant Soil 49, 533-550.

Schmitz, G.H., Puhlmann, H., Droge, W., Lennartz, F., 2005. Artificial neural networks for estimating soil hydraulic parameters from dynamic flow experiments. Eur. J. Soil Sci. 56, 19-30.

Šimunek, J., Vogel, T., Van Genuchten, M.Th., 1992. The SWMS_2D code for simulating water flow and solute transport in two-dimensional variably saturated media, v 1.1, Research Report No. 126, U. S. Salinity Lab, ARS USDA, Riverside.

Šimůnek J., van Genuchten M.Th., Šejna M., 2005. The HYDRUS-1D software package for simulating the one-dimensional movement of water, heat, and multiple solutes in variably-saturated media. Version 3.0. HYDRUS Softw. Ser. 1. Department of Environmental Sciences, University of California, Riverside, CA.

Šimůnek, J., van Genuchten M.Th., Šejna M. 2006. The HYDRUS software package for simulating two- and three-dimensional movement of water, heat, and multiple solutes in variably-saturated media: Technical manual. Version 1.0. PC-Progress, Prague, Czech Republic.

Šimůnek J., Van Genuchten M.Th., Šejna M., 2008. Development and applications of the HYDRUS and STANMOD software packages and related codes. Vadose Zone J. 7, 587–600.

Sonnleitner, M.A., Abbaspour, K.C., Schulin, R., 2003. Hydraulic and transport properties of the plant–soil systems estimated y inverse modelling. Eur. J. Soil Sci. 54, 127-138.

Steduto, P., Hsiao, T.C., Raes, D., Fereres, E., 2009. AquaCrop - The FAO crop model to simulate yield response to water: I. Concepts and underlying principles. Agron. J. 101, 426-437.

Thorup-Kristensen, K., 2006. Root growth and nitrogen uptake of carrot, early cabbage, onion and lettuce following a range of green manures. Soil Use Manage. 22, 29-38.

Van Genuchten, M.Th., 1980. A closed-form equation for predicting the hydraulic conductivity of unsaturated soils. Soil Sci. Soc. Am. J. 44, 892-898.

Van Genuchten, M.Th., Leij, F.J., Yates, S.R., 1991. The ReTC code for quantifying the hydraulic functions of unsaturated soils. Robert S. Kerr Environmental Research Laboratory, U. S. Environmental Protection Agency, Oklahoma, USA.

Whitfield, W.A.D., 1974. The soils of the National Vegetable Research Station, Wellesbourne. Rep. Natn. Veg. Res. Stn for 1973, The British Society for the promotion of vegetable research Wellesbourne UK, pp.21-30.

Wösten, J.H.M., Lilly, A., Nemes, A., Le Bas, C., 1999. Development and use of a database of hydraulic properties of European soils. Geoderma 90, 169-185.

Wu, J., Zhang, R., Gui, S., 1999. Modeling soil water movement with water uptake by roots. Plant Soil 215, 7-17.

Yang, D., Zhang, T., Zhang, K., Greenwood, D.J., Hammond, J., White, P.J., 2009. An easily implemented agro-hydrological procedure with dynamic root simulation for water transfer in the crop-soil system: validation and application. J. Hydrol. 370, 177-190.

Zhang, K., Greenwood, D.J., White, P.J., Burns, I.G., 2007. A dynamic model for the combined effects of N, P and K fertilizers on yield and mineral composition; description and experimental test. Plant Soil 298, 81-98.

Zhang, K., Yang, D., Greenwood, D.J., Rahn, C.R., Thorup-Kristensen, K., 2009. Development and critical evaluation of a generic 2-D agro-hydrological model (SMCR_N) for the responses of crop yield and nitrogen composition to nitrogen fertilizer. Agric. Ecosyst. Environ. 132, 160-172.

Table 1: Physical properties of the soil profile

Depth (cm)	% Sand (2~0.02 mm)	% Silt (0.02~0.002 mm)	%Clay (<0.002 mm)	Organic matter (%)	Bulk density (g cm^{-3})	Water content at field capacity (cm^3 cm^{-3})
0.0 ~ 3.8	76	9	15	5.1	1.55	0.24
3.8 ~ 7.5	75	9	16	5.5	1.56	0.24
7.5 ~ 11.3	75	9	16	5.4	1.61	0.25
11.3 ~ 15.0	75	9	16	6.0	1.66	0.25
15.0 ~ 18.8	75	9	16	5.8	1.72	0.27
18.8 ~ 22.5	75	10	15	5.3	1.75	0.29
22.5 ~ 26.3	75	10	15	1.3	1.76	0.28
26.3 ~ 30.0	74	10	16	1.5	1.74	0.29
30.0 ~ 33.8	74	10	16	2.8	1.70	0.28
33.8 ~ 37.5	77	9	14	3.8	1.65	0.25
37.5 ~ 41.3	78	9	13	3.0	1.59	0.23
41.3 ~ 45.0	79	8	13	2.3	1.56	0.21

Table 2: Deduced soil water characteristics using different fitness functions and population sizes, and statistical assessment for resulting soil water content data

Fitness	Population size	θ_s (cm^3 cm^{-3})	α (cm^{-1})	n	θ_r (cm^3 cm^{-3})	K_s (cm day^{-1})	RMSE (cm^3 cm^{-3})	MAE (cm^3 cm^{-3})	EF
$-\Sigma(\theta_{mea}-\theta_{sim})^2/N$	5	0.332	0.1128	1.131	0.0027	49.0	0.0227	0.0182	0.547
	10	0.422	0.0955	1.198	0.0078	118.2	0.0225	0.0186	0.556
$-\Sigma(\theta_{mea}-\theta_{sim})^2/N-(\theta_{FC\_mea}-\theta_{FC\_sim})^2$	5	0.425	0.0636	1.185	0.0544	225.7	0.0237	0.0190	0.504
	10	0.425	0.0506	1.205	0.0635	134.7	0.0240	0.0194	0.495

EF: modelling efficiency coefficient; RMSE: root of the mean squared errors; MAE: mean absolute error.

Figure captions

Figure 1: Sensitivity analyses of soil hydraulic parameters for the calibration experiment. The model response in the *y* axis is the mean square residuals of soil water content between measurement and simulation. The symbols □, ×, *, ◊ and Δ represent soil hydraulic parameters, θ_s, θ_r, α, n and K_s, respectively, with the values set as 0.336 $cm^3\ cm^{-3}$, 0.025 $cm^3\ cm^{-3}$, 1.218, 0.04869 and 28.88 cm d^{-1} derived from PTFs proposed by Wosten et al. (1999).

Figure 2: Measured daily rainfall (a) and calculated potential evaporation using the FAO approach (b) from Day 117 (27/04/71) to Day 325 (21/11/71) in the calibration experiment.

Figure 3: Measured daily rainfall (a) and calculated potential evapotranspiration using the FAO approach (b) from Day 220 (08/08/73) to Day 246 (03/09/73) in the verification experiment.

Figure 4: Soil water retention curves deduced using a GA and calculated with other alternatives. The upper lines with the symbols □ and ◇ are the curves deduced using population sizes of 5 and 10 with a hybrid fitness function, respectively. The lower solid and dotted lines are derived from PTFs proposed by Wosten et al. (1999) and Cresswell et al. (2006), respectively. Soil water content at saturation for the curve from Cresswell et al. (2006) is assumed the same as that from Wosten et al. (1999).

Figure 5: Overall comparison of soil water content between measurement and simulation in the calibration experiment.

Figure 6: Soil water contents measured and simulated using the deduced soil hydraulic properties down the soil profile in the calibration experiment. Solid line represents the simulations and the symbol Δ represents measurements.

Figure 7: Cumulative rainfall, potential and actual evaporation during the calibration experiment.

Figure 8: Simulated soil water contents in different layers (a) and water flux at the lower boundary (b) during the calibration experiment.

Figure 9: Averaged relative root density distribution (means and dispersions) of leek measured on Day 220 (08/08/73) and Day 246 (03/09/73) down the soil profile (a) and the measured soil water content down the profile on 08/08/73, and the measured and simulated soil water content on 03/09/73 (b). The solid line in (a) represents fitted relative root density distribution using exponential functions and the symbol Δ represents the measurements. The symbols □ and Δ in (b) represent the measured soil water content distributions on 08/08/73 and 03/09/73, respectively, and the solid line represents the simulated water content distributions on 03/09/73 using the soil water hydraulic properties deduced in this study.

Figure 10: Simulated root water uptake (a) and soil water content (b) in different soil layers from Day 220 (08/08/73) to Day 246 (03/09/73) in the verification experiment.

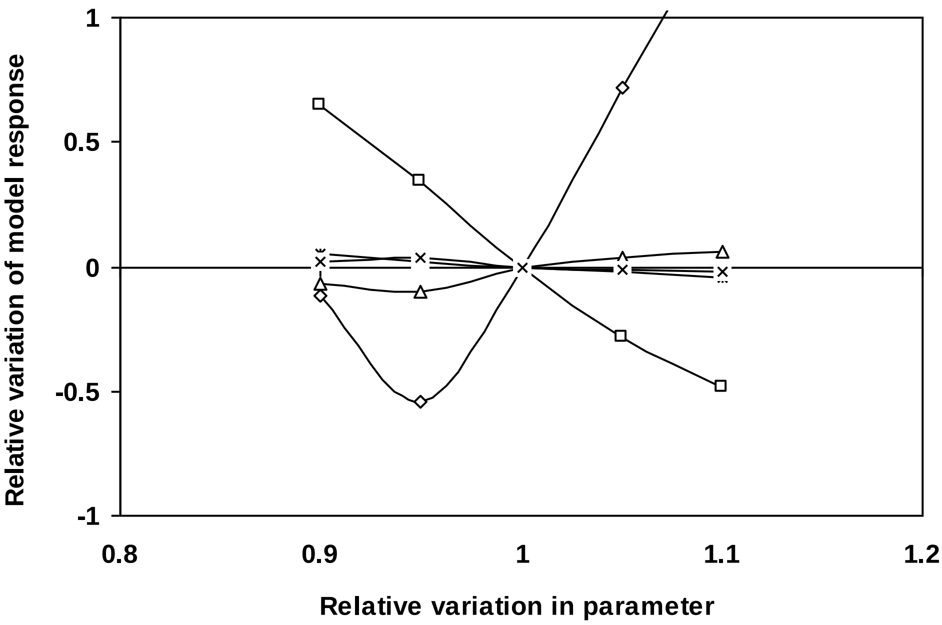
1
0.5
0
-0.5
-1
0.8
0.9
1
1.1
1.2
Relative variation of model response
Relative variation in parameter

Figure 1

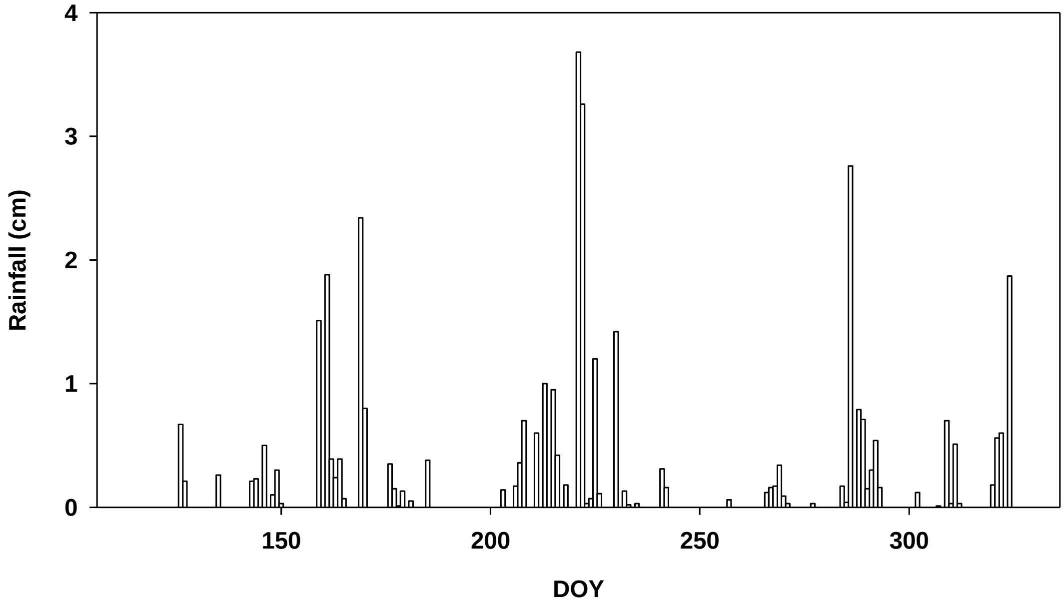
4
3
2
1
0
Rainfall (cm)
150
200
250
300
DOY

(a)

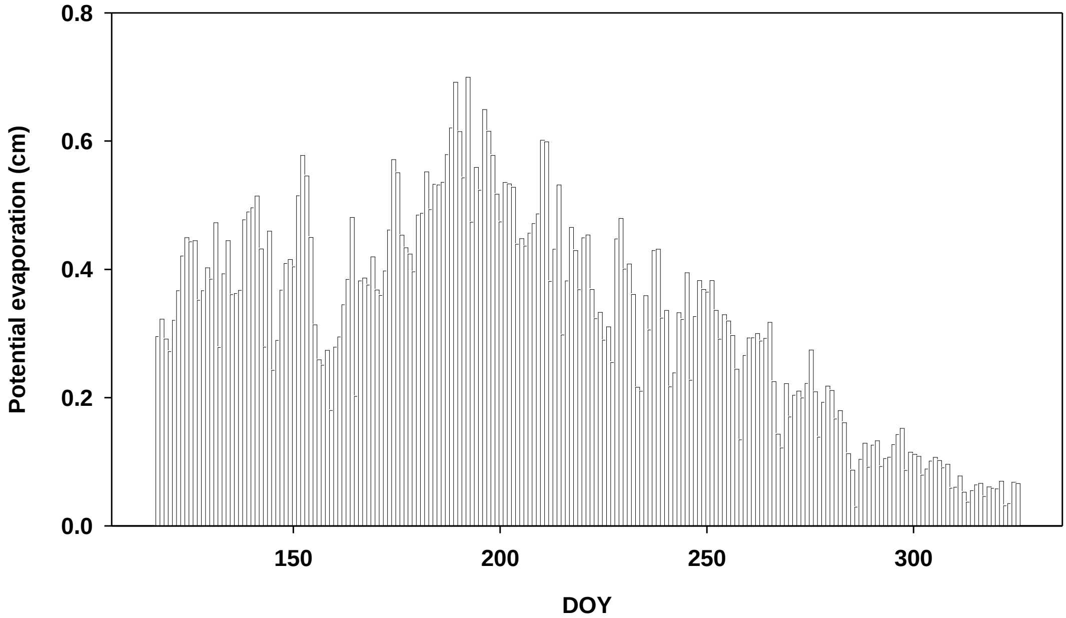
0.8
0.6
0.4
0.2
0.0
Potential evaporation (cm)
150
200
250
300
DOY

(b)

Figure 2

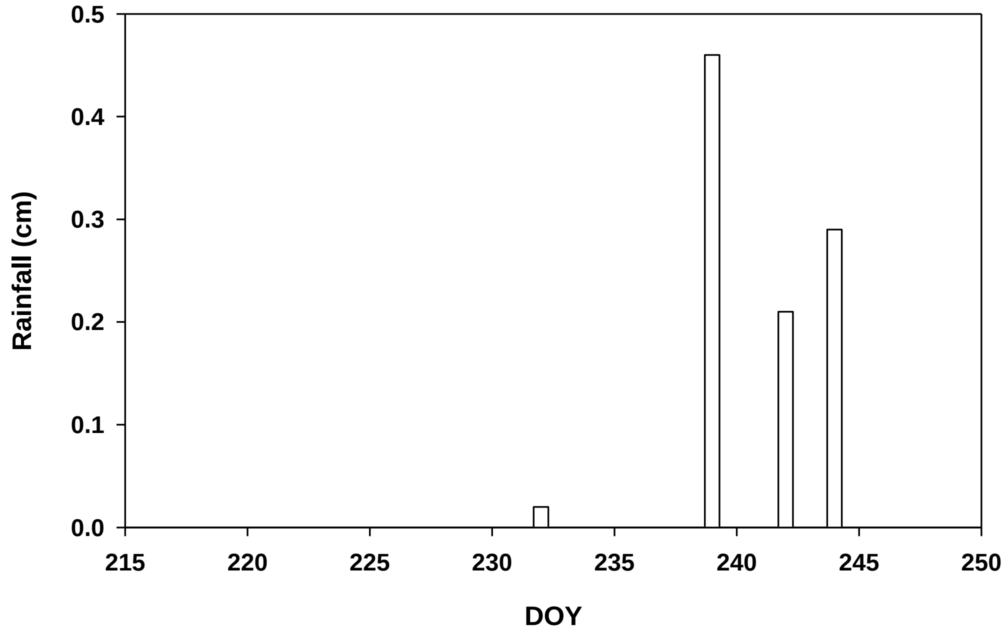
0.5
0.4
0.3
0.2
0.1
0.0
Rainfall (cm)
215
220
225
230
235
240
245
250
DOY

(a)

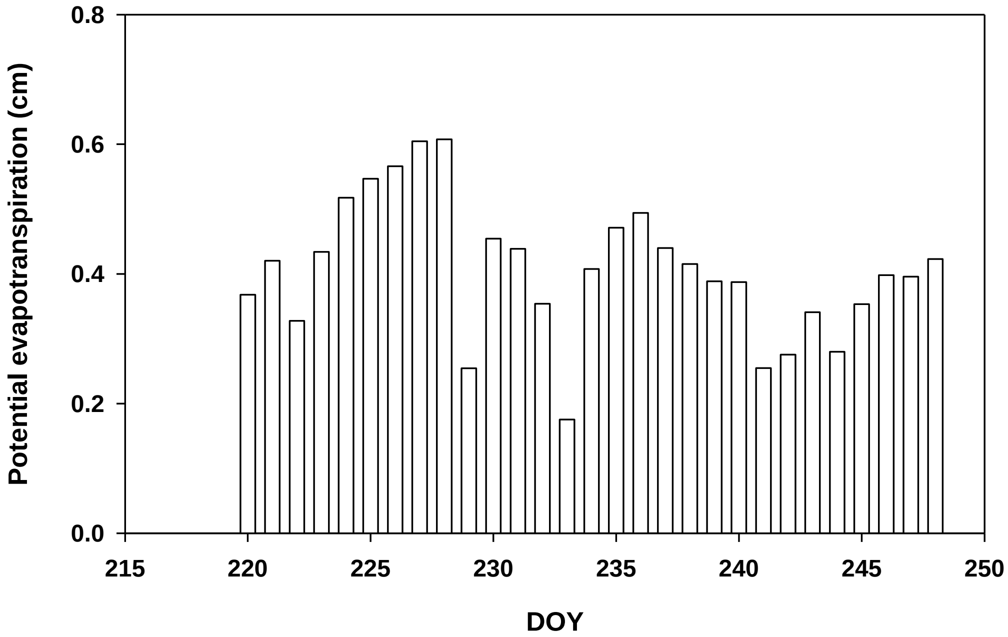
0.8
0.6
0.4
0.2
0.0
Potential evapotranspiration (cm)
215
220
225
230
235
240
245
250
DOY

(b)

Figure 3

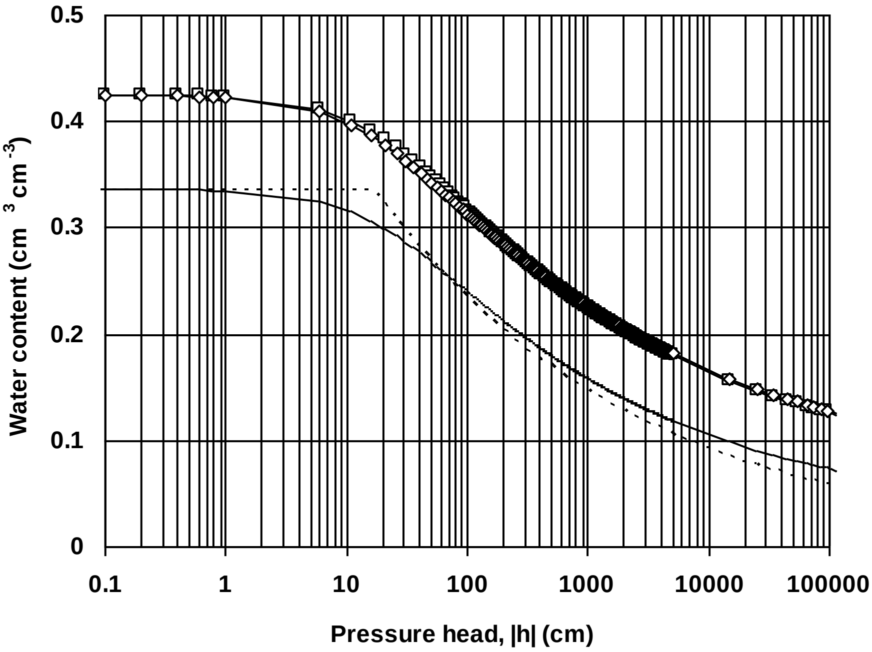

0.5
0.4
0.3
0.2
0.1
0
Water content (cm 3 cm -3)
0.1
1
10
100
1000
10000
100000
Pressure head, |h| (cm)

Figure 4

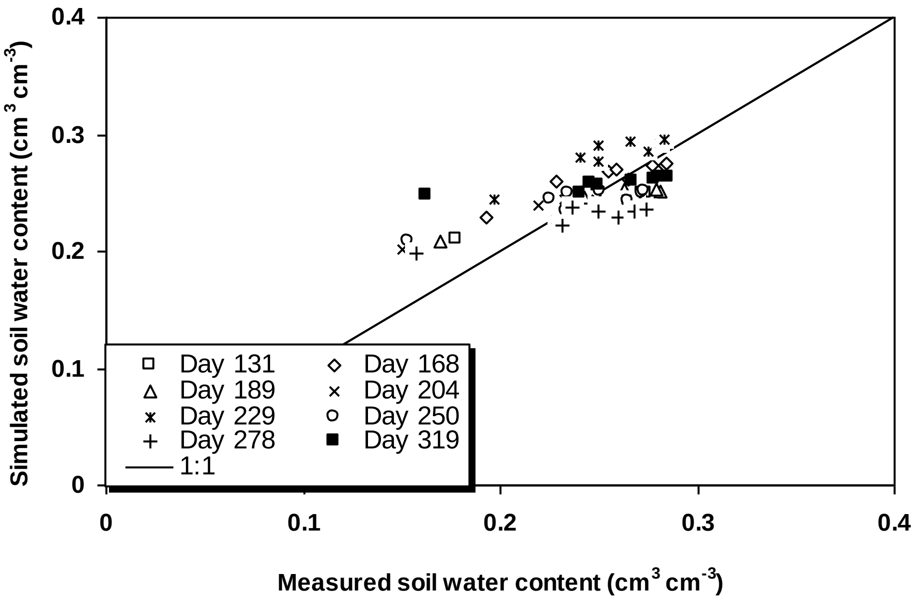

Simulated soil water content (cm^3 cm^{-3})
0.4
0.3
0.2
0.1
0
0
0.1
0.2
0.3
0.4
Measured soil water content (cm^3 cm^{-3})
Day 131
Day 168
Day 189
Day 204
Day 229
Day 250
Day 278
Day 319
1:1

Figure 5

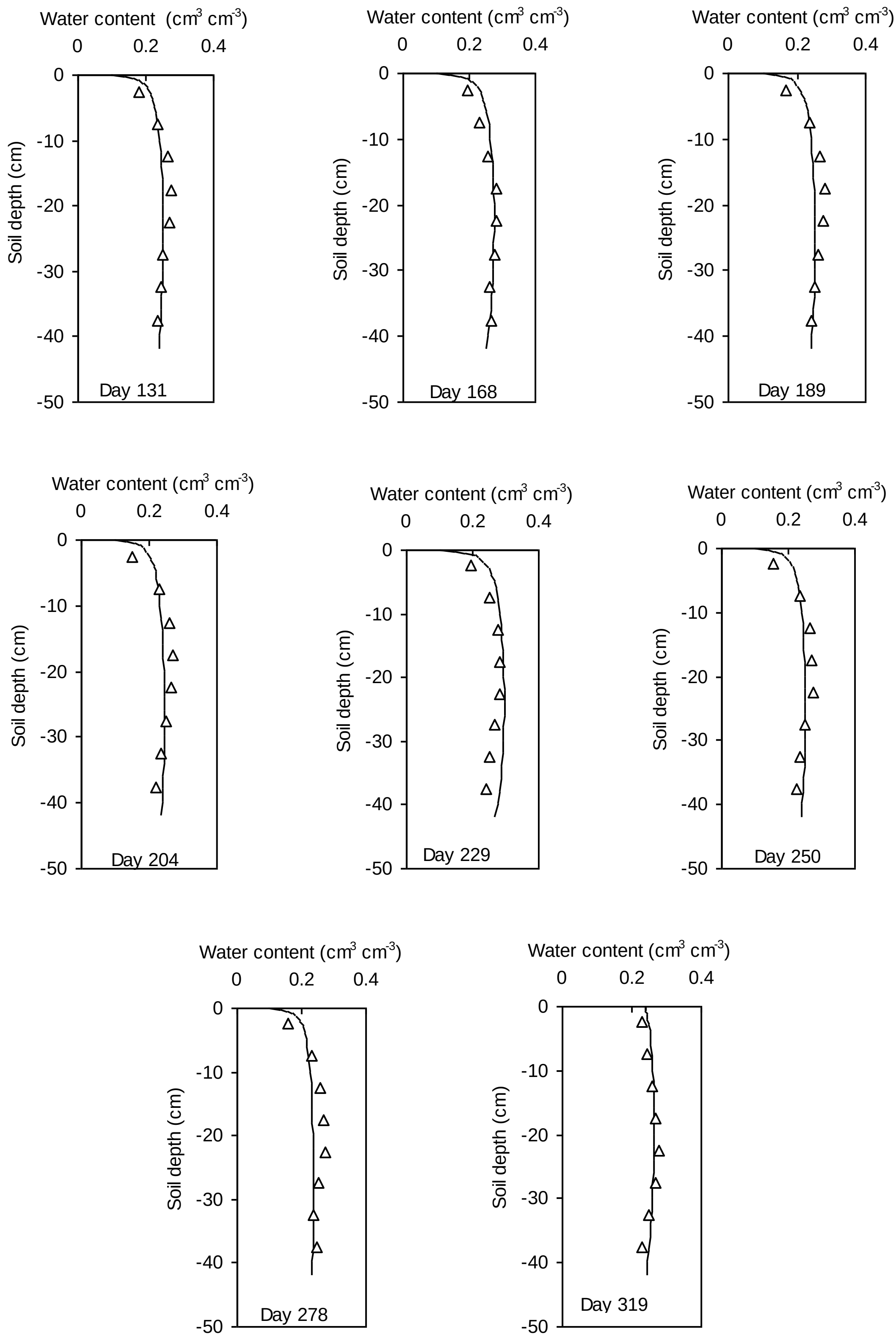

Water content (cm3 cm-3)
0
0.2
0.4
Soil depth (cm)
0
-10
-20
-30
-40
-50
Day 131
Day 168
Day 189
Day 204
Day 229
Day 250
Day 278
Day 319

Figure 6

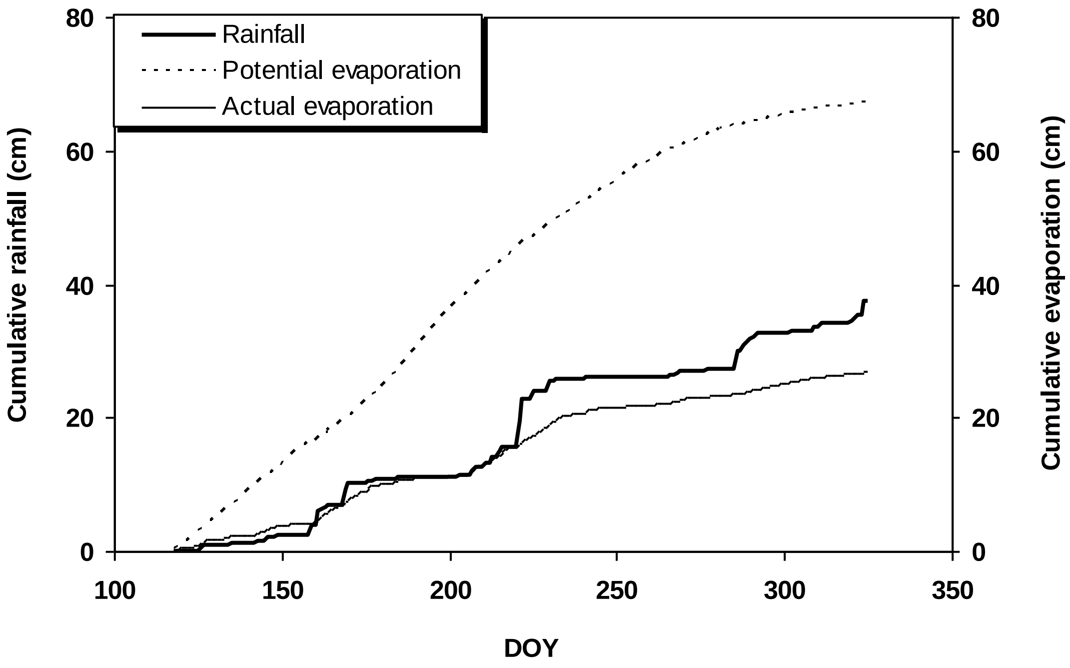

Rainfall
Potential evaporation
Actual evaporation
Cumulative rainfall (cm)
Cumulative evaporation (cm)
DOY
0
20
40
60
80
100
150
200
250
300
350

Figure 7

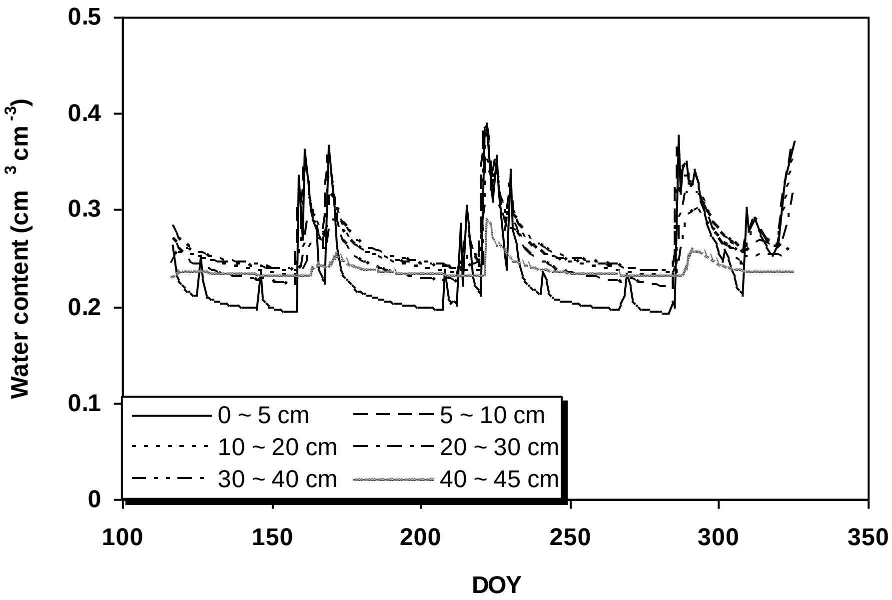

Water content (cm 3 cm -3)
0.5
0.4
0.3
0.2
0.1
0
100
150
200
250
300
350
DOY
0 ~ 5 cm
5 ~ 10 cm
10 ~ 20 cm
20 ~ 30 cm
30 ~ 40 cm
40 ~ 45 cm

(a)

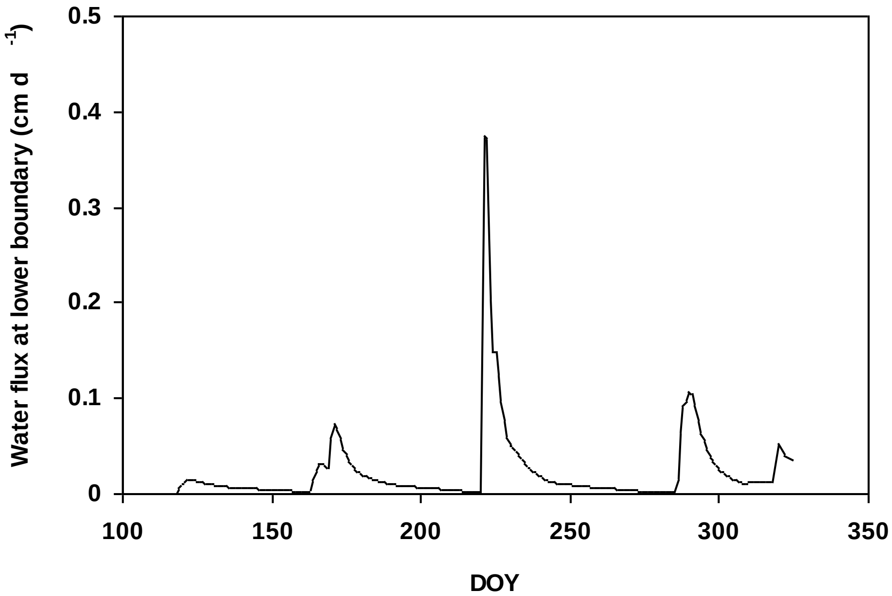

Water flux at lower boundary (cm d -1)
0.5
0.4
0.3
0.2
0.1
0
100
150
200
250
300
350
DOY

(b)

Figure 8

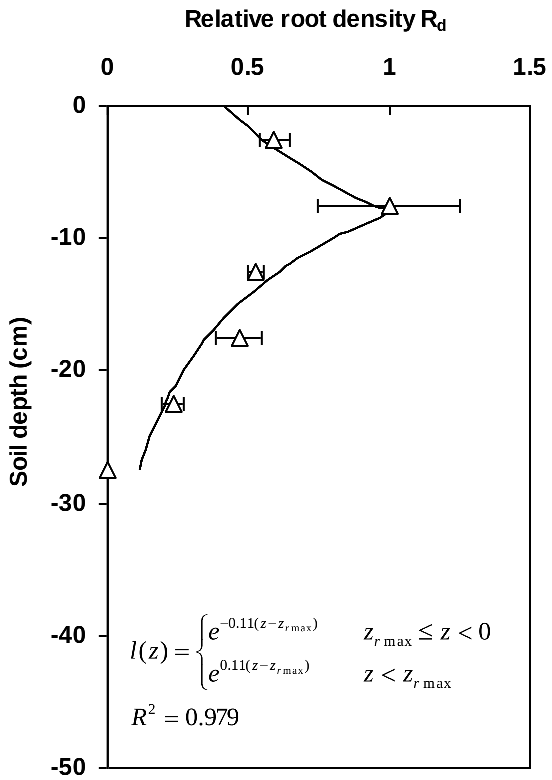
Relative root density R_d
0
0.5
1
1.5
0
-10
-20
-30
-40
-50
Soil depth (cm)
$l(z) = \begin{cases} e^{-0.11(z - z_{r\max})} & z_{r\max} \le z < 0 \\ e^{0.11(z - z_{r\max})} & z < z_{r\max} \end{cases}$
$R^2 = 0.979$

(a)

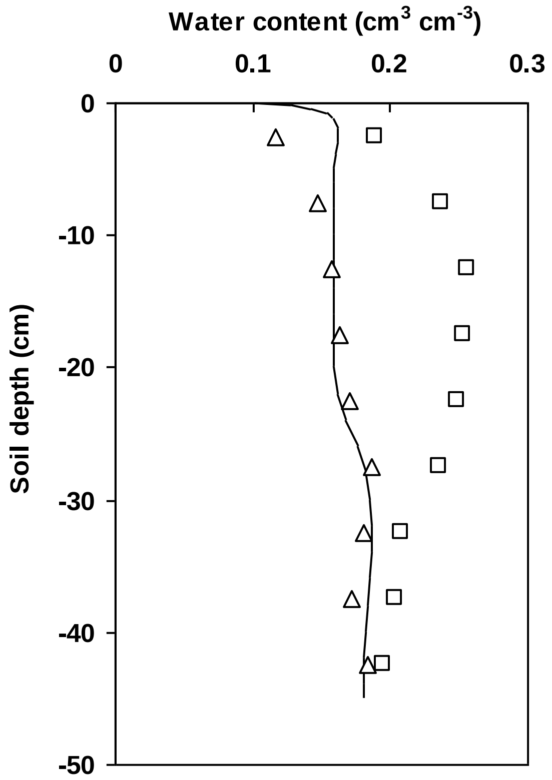
Water content ($cm^3\ cm^{-3}$)
0
0.1
0.2
0.3
0
-10
-20
-30
-40
-50
Soil depth (cm)

(b)

Figure 9

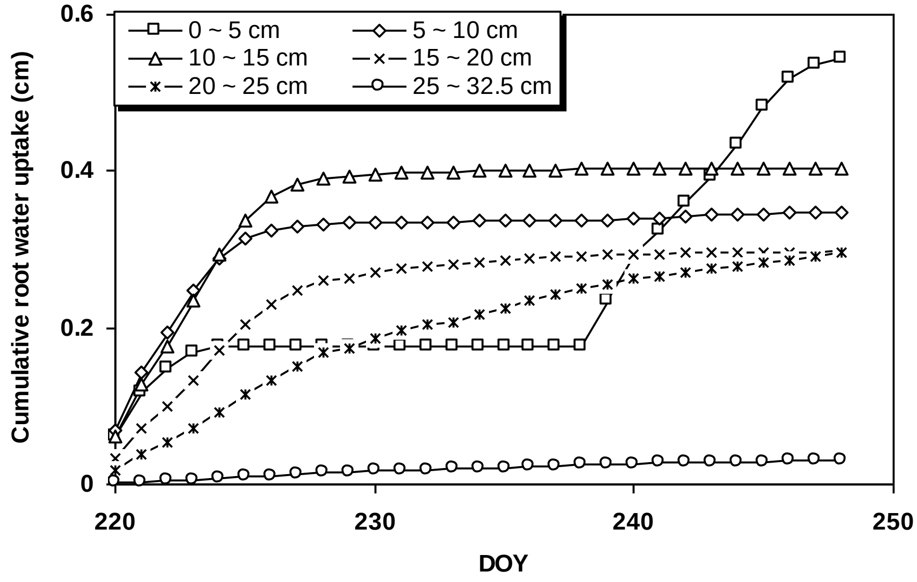
0 ~ 5 cm
5 ~ 10 cm
10 ~ 15 cm
15 ~ 20 cm
20 ~ 25 cm
25 ~ 32.5 cm
Cumulative root water uptake (cm)
0.6
0.4
0.2
0
220
230
240
250
DOY

(a)

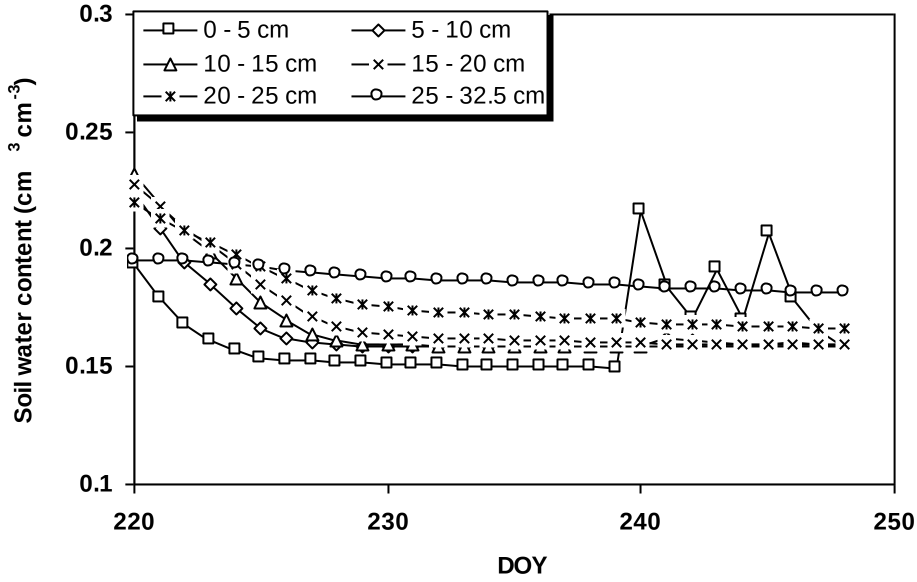
0 - 5 cm
5 - 10 cm
10 - 15 cm
15 - 20 cm
20 - 25 cm
25 - 32.5 cm
Soil water content (cm 3 cm -3)
0.3
0.25
0.2
0.15
0.1
220
230
240
250
DOY

(b)

Figure 10